*Original*

Lang, S.; Lee, H.S.; Petrov, A.Y.; Stoermer, M.; Ritter, M.; Eich, M.:
**Gold-silicon metamaterial with hyperbolic transition in near infrared**
In: Applied Physics Letters (2013) AIP

DOI: 10.1063/1.4813499

# Gold-silicon metamaterial with hyperbolic transition in near infrared

S. Lang,[1,a)] H. S. Lee,[1] A. Yu. Petrov,[1] M. Störmer,[2] M. Ritter,[3] and M. Eich[1]
[1]*Institute of Optical and Electronic Materials, Hamburg University of Technology, 21073 Hamburg, Germany*
[2]*Institute of Materials Research, Helmholtz-Zentrum Geesthacht Centre for Materials and Coastal Research, Max-Planck-Straße 1, 21502 Geesthacht, Germany*
[3]*Electron Microscopy Unit, Hamburg University of Technology, 21073 Hamburg, Germany*

(Received 25 April 2013; accepted 25 June 2013; published online 10 July 2013)

In this paper, we focus on the creation and characterization of a hyperbolic metamaterial for near infrared. To shift the hyperbolic transition there, a stack of alternating 7 nm gold and 42 nm silicon layers is chosen. Samples are manufactured using magnetron sputtering and different measurements confirm their structure. We fit the Drude model of gold to reproduce measured reflectivity and transmittance by simulations. The collision frequency of the thin film gold is increased by 9 times, which shifts the transition of our metamaterial to the hyperbolic regime to even larger wavelengths. The performance is comparable to other proposed metamaterials. © *2013 AIP Publishing LLC*. [http://dx.doi.org/10.1063/1.4813499]

Metamaterials are artificially created, structured materials with unique properties.[1–3] A special class of metamaterials is hyperbolic metamaterials (HMMs).[4–6] They are a good approximation of hyperbolic media[2,7] which, for the uniaxial case, have a permittivity tensor

$$\begin{pmatrix} \varepsilon_x & 0 & 0 \\ 0 & \varepsilon_x & 0 \\ 0 & 0 & \varepsilon_z \end{pmatrix} \tag{1}$$

with $\Re(\varepsilon_x) \times \Re(\varepsilon_z) < 0$ but have not been found for optical frequencies yet. HMMs are of interest because of the negative refraction they can show[8] and because of their support of waves with high k vector magnitudes along certain directions.[9] Systems consisting of alternating layers of a dielectric and a metal are one possible realization.[5,8,10] Ref. 4 gives a good overview of the topic of HMMs.

Popular metals for HMMs and other metamaterials are gold and silver. But fabrication difficulties, high losses and large negative real parts of permittivity in the near infrared (NIR) have raised the search for better plasmonic materials[11,12] for this wavelength range. These are materials with metal like behavior but smaller concentration of free carriers. The NIR region is interesting for optical communication as well as for thermophotovoltaic applications.[13,14] Promising candidates are transparent conducting oxides (TCOs)[15] and transition-metal nitrides.[16]

The aim of this work is to create a metamaterial with a transition to the hyperbolic region in the NIR using conventional metals. Transition means that the effective permittivity of the hyperbolic metamaterial is frequency dependent and that the HMM is actually a HMM only in a certain wavelength region, whereas for other wavelengths the HMM behaves like a conventional material. The reason for that is the strong frequency dependence of $\varepsilon$ of the plasmonic material. We use very thin layers of metal and relatively thick dielectric layers to compensate for the large negative permittivity.

We choose a layered system of gold and silicon. Despite common notion, we will show that a HMM made of gold can still perform in NIR. The relative permittivity of gold can be described by the Drude model[11]

$$\varepsilon_{Au} = \varepsilon_\infty - \frac{(2\pi f_p)^2}{\omega(\omega + i\omega_{col})}. \tag{2}$$

Fitting that to the values measured by Johnson and Christy[17] at NIR one finds out that $\varepsilon_\infty = 8.2$, $f_p = 2152$ THz, and $\omega_{col} = 106$ THz, at least for bulk gold. We assume for the silicon a refractive index of 3.5 with negligible loss compared to metal. Values in literature[18,19] are close to that for wavelengths larger than 1.2 $\mu$m. The multilayers have been deposited on a double polished silicon substrate of 0.5 mm thickness.

To understand our idea, let us recall the formulas for the effective medium[5]

$$\varepsilon_x = \varepsilon_y = \frac{d_M\varepsilon_M + d_D\varepsilon_D}{d_M + d_D}, \tag{3}$$

$$\frac{1}{\varepsilon_z} = \frac{\frac{d_M}{\varepsilon_M} + \frac{d_D}{\varepsilon_D}}{d_M + d_D}. \tag{4}$$

The thicknesses and permittivities of the layers are defined by $d$ and $\varepsilon$, where the indices "$D$" and "$M$" stand for dielectric and metal, respectively. The layers are assumed to alter along the $z$-direction.

The real part of $\varepsilon_M$ decreases with wavelength. Since the permittivity of a dielectric is positive and constant compared to the metal, $\varepsilon_x$ is just a scaled and shifted version of $\varepsilon_M$. The shift is in direction of higher values. At some point, the real part of $\varepsilon_x$ will change the sign from positive for small wavelengths to negative for higher wavelengths. If this transition point is supposed to be in NIR the large, negative dielectric constant of gold must be compensated for. This is why we choose silicon as the dielectric. $\varepsilon_z$ is dominated by $\varepsilon_D$ in near infrared.

The second issue involves the thicknesses of layers. By changing them, the transition point can also be shifted.

a)Electronic mail: slawa.lang@tuhh.de

 

Putting less metal makes the curve flatter and shifts it more. There is an additional positive effect of making the dielectric thicker. The average losses of the HMM become lower. From Eqs. (3) and (4), it is obvious: the less $\varepsilon_M$ is weighted the lower the imaginary part of the effective permittivity and the lower the losses.

All samples have been fabricated using a magnetron sputtering technique for layer by layer deposition. The Au/Si layers have been produced on planar, well-polished silicon substrates in an ultrahigh-vacuum chamber by DC (gold) and medium frequency (silicon) magnetron sputtering. The deposition chamber has comprised two magnetron sources with diameters of 3 in. The water-cooled substrate holder has been rotated in order to achieve uniform film thickness. A computer-driven shutter between the targets and substrate has controlled the deposition time. The deposition rates of Si and Au have been 0.18 and 0.38 nm/s, respectively. The sputtering gas has been high purity argon 7.0 (i.e., 99.99999%, purchased from Linde, Germany) with a pressure of 0.2 Pa, whereas the typical background pressure in the deposition chamber has been less than $10^{-5}$ Pa.

The gold layers should be as thin as possible to increase the dielectric-to-metal thickness ratio and to make it a metamaterial with good effective medium properties at NIR. Metamaterials should have structure sizes significantly below the wavelength in the material. Because $|\varepsilon_{Au}|$ is large, the wavelength in gold is much shorter than in air. On the other hand, manufacturing very thin layers is difficult. Especially, preventing island formation is challenging. The fabricated sample has got $d_{Au} \approx 7$ nm. Samples with smaller thickness of gold were unstable and tended to island formation.

Increasing the $d_{Si}$ to $d_{Au}$ ratio must be traded off against the desired small structure size of metamaterials to decide on $d_{Si}$. The choice was made to $d_{Si} \approx 42$ nm resulting in $d_{Si}/d_{Au} \approx 6$. The exact architecture of the sample is the following: On a double polished, 500 $\mu$m thick silicon wafer 13 layers of gold and 12 layers of silicon have been deposited. The first layer on the substrate is gold. Then silicon and gold follow by turns such that the last layer is again gold.

X-ray reflectometry (XRR) and scanning electron microscopy (SEM) both confirm that gold and silicon have not mixed up. They form a layered system. Fig. 1 shows a XRR measurement together with a fit. The measurement was performed with copper K-$\alpha$ radiation using an x-ray reflectometer (D8 Advance, Bruker) equipped with a reflectometry stage and a primary Göbel mirror. The resulting curves were fitted using the simulation software LEPTOS in order to determine the multilayer period, density and roughness. The inset is a SEM picture of the layered structure. The clear periodicity is an indicator for the structure. The roughness can be estimated to be small.

To be able to determine the permittivity of our HMM transmission and reflection of the sample have been measured. A Fourier transform infrared (FTIR) spectroscope, model Tensor 37 from Bruker Company, was used. The wavelength range was from 1.2 $\mu$m to 4 $\mu$m. At $\lambda = 1.7$ $\mu$m, the setup (detector, beam splitter, source) has to be swapped. As a result, a small jump occurs in the curves at that position, which has no meaning in the context of this paper.

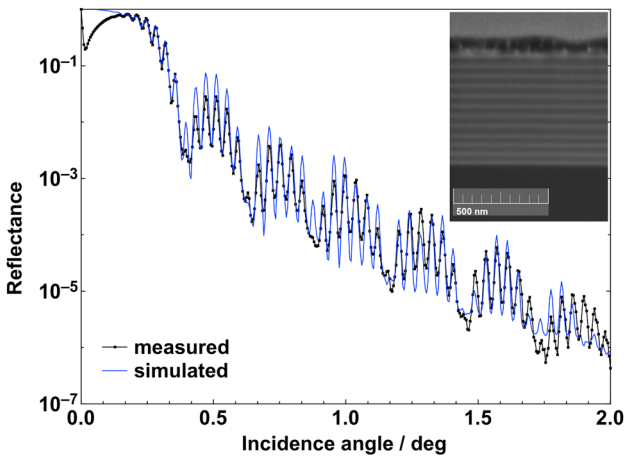


FIG. 1. XRR measurement together with a fitted simulation. Both coincide well. Inset: SEM picture of fabricated sample. The multilayer stack located on a silicon substrate is featured here. Because of charging effects the upper surface seems rough.

Transmission was measured only for normal incidence, where the polarization is indifferent. The reflectivity was measured for the angles of incidence $\varphi$ from 15° to 60° in 5° steps. S- and p-polarizations were distinguished.

The first thing we did was to take the whole structure of the sample into account. The method of choice for layered structures is the transfer-matrix method (TMM). The measured results could not be reproduced with bulk gold properties. A possible explanation for discrepancy is the increase of the collision frequency of gold $\omega_{col}$ in thin layers. Different research groups have found out that in thin metallic layers, the material tends to cluster and therefore $\omega_{col}$ becomes significantly larger.[11,20,21]

Two fits have been performed. One where only $\omega_{col}$ and another where all three Drude model parameters have been adjusted such that the error

$$\sum_{\lambda} \sum_{\varphi_s,\varphi_p} \left( \frac{R_m - R_{th}}{R_m} \right)^2 + \sum_{\lambda} w \left( \frac{T_m - T_{th}}{T_m} \right)^2 \qquad (5)$$

is minimized. Subscripts "*m*" and "*th*" stand for measured and simulated (theoretical) values. 86 equidistant wavelength points between 1.2 $\mu$m and 4 $\mu$m have been used. We have weighted $T$ by $w = 0.1$. The noise which is strong because of weak transmission should not influence the fit too much.

The fit where only $\omega_{col}$ is adjusted—"fit 1"—has resulted in $\omega_{col} = 1109$ THz (1048–1168 THz) (assuming $\varepsilon_\infty = 8.2$, $f_p = 2152$ THz), the other one—"fit 3"—has resulted in $\varepsilon_\infty = 6.9$ (2.8–11.5), $f_p = 2005$ THz (1972–2039 THz) and $\omega_{col} = 932$ THz (882–981 THz). The values in brackets give the parameter ranges in which the error is below 110% of the minimal error. The figure 110% is chosen arbitrarily here. To get the ranges for "fit 3," only one parameter was varied at a time, while the other two were set to the values in front of their brackets (optimal values).

Collision frequency is significantly increased in both cases. In Fig. 2, the measured transmission together with the simulated transmissions for the fitted parameter values can be seen. "Fit 3" is obviously better capturing the transmission measurement and its values for $\varepsilon_\infty$ and $f_p$ can still be

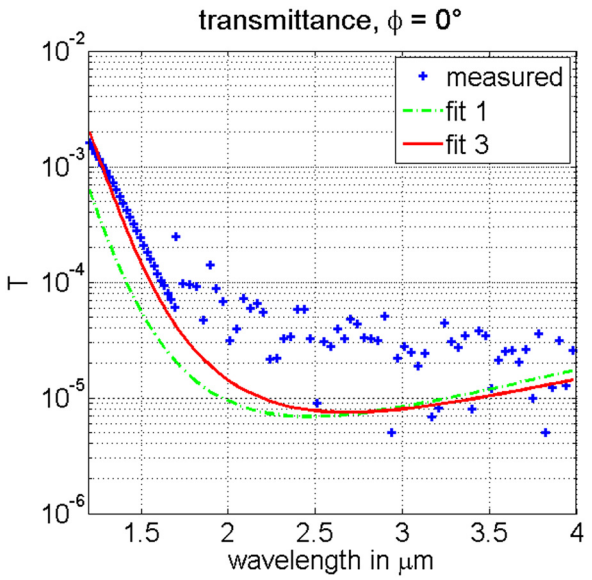


FIG. 2. Measured and simulated normal transmission. For the simulation, the fitted parameters have been used. In "fit 1," only collision frequency, in "fit 3," all three parameters have been adjusted.

called bulk values. Fig. 3 shows examples of the reflection. As in Fig. 2, the two fits are shown together with the measurement. Here, both fits are equally good. There is still some discrepancy in the shape and position of the fitted and measured curves. This can be explained by the limitation of the Drude model fit. In the following discussion, we will only use the better "fit 3."

The effect of the changed collision frequency on the effective permittivity of the metamaterial can be seen in Fig. 4. The figure separates real (Fig. 4(a)) and imaginary parts (Fig. 4(b)). $\varepsilon_z$ is dominated by the permittivity of silicon. $\varepsilon_x$ is a narrowed, then shifted version of $\varepsilon_{Au}$. When $\omega_{col}$ becomes larger, the magnitude of the imaginary part increases leading to higher losses. In many cases that is undesired but in some applications like enhanced near field heat transfer[13,22] or enhanced spontaneous emission,[23,24] a certain level of absorption is desirable. Besides that also the magnitude of the real part of $\varepsilon_{Au}$ is decreased. Thus, the increase in collision frequency not only changes the losses but also helps shifting the transition point to near infrared. The result is a flatter curve for $\varepsilon_x$ with a transition point at

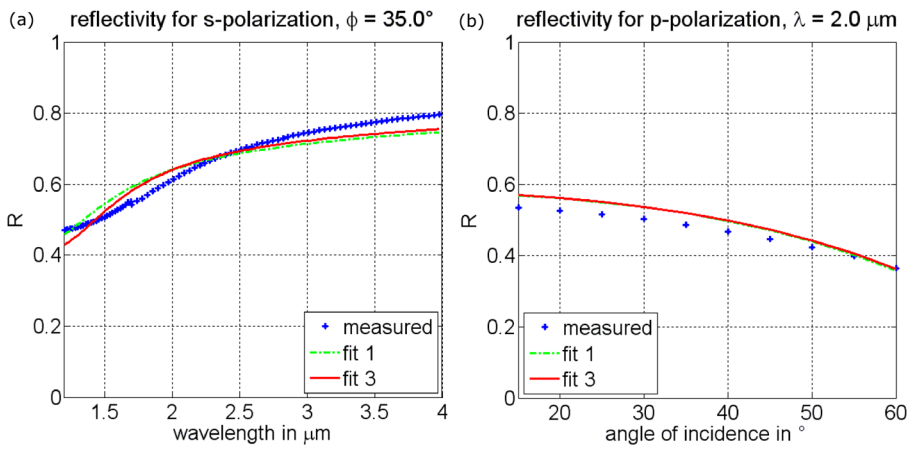


FIG. 3. Measured and simulated reflection. Two exemplary curves are shown. (a) Reflection for a fixed angle of incidence 35°, s-polarization. (b) Reflection for a fixed wavelength 2 $\mu$m, p-polarization.

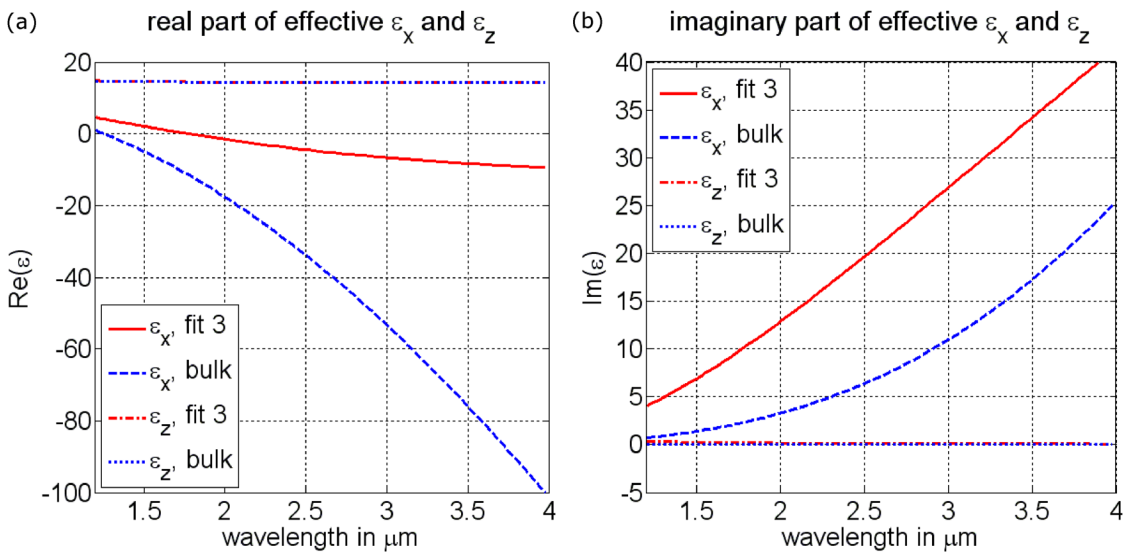


FIG. 4. Effective permittivities of our HMM calculated with effective medium theory. (a) Shows the real parts and (b) the imaginary parts. For comparison, not only the values for thin film gold ("fit 3") but also values for bulk gold ("bulk") are displayed.

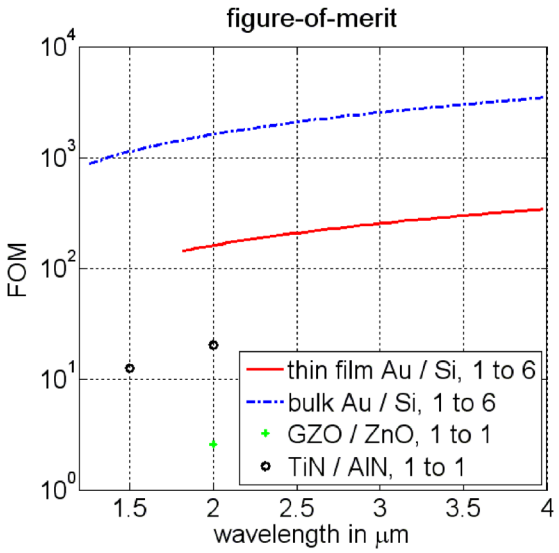


FIG. 5. Figure-of-merit of HMMs. Our metamaterial is shown with thin film gold as analyzed and assuming bulk gold properties. Besides, two other HMM systems are shown, namely, GZO/ZnO and TiN/AlN having equal layer thicknesses.

longer wavelengths. If intended, the point can be shifted back by changing the thicknesses ratio.

To compare our hyperbolic metamaterial with others, we use a figure-of-merit (FOM) which is commonly used for HMMs designed for negative refraction. It is the ratio of real and imaginary part of $k_z$ assuming $k_x = k_y = 0$.[8] The layered system is considered as an effective medium here. This definition makes sense as long as the hyperbola in the ($k_x$ - $k_z$)-plane intersects the $k_z$-axis and not the $k_x$-axis. When the hyperbola is rotated by 90°, as in our case, the definition must be adjusted otherwise the FOM would be 0 for a lossless material. We make it simple and take real and imaginary part of $k_x$ assuming $k_z = k_y = 0$ in this case. Thus, this definition is not connected to the orientation of the sample but connected to the orientation of the hyperbola. However, because the layers are oriented orthogonally, a direct comparison of systems with different hyperbola orientations is difficult and should be avoided.

As can be seen in Fig. 5, our FOM is smaller than it would be with bulk gold approximation. Despite larger collision frequency, the FOM of the presented metamaterial is still larger than the FOM of HMMs consisting of NIR plasmonic materials like TiN or gallium-doped ZnO (GZO). The thicknesses of plasmonic and dielectric materials in those HMMs are assumed to be equal and the permittivities are taken from Refs. 12 (plasmonic materials) and 25 (dielectrics). Orientation of the hyperbola is the same for all systems shown in Fig. 5, which makes them comparable.

In conclusion, we have demonstrated the possibility to create a NIR metallic hyperbolic metamaterial that does not need special NIR plasmonic materials. It has still a large FOM in comparison to other HMMs with these materials. The approach is based on a combination of thin metal layers and high refractive index dielectric layers.

We have also found out that the often neglected increase of collision frequency in thin metallic layers is a significant effect. It must be taken into account if layer thicknesses come in the range of a few nanometers. In our case, increased collision frequency of thin metal films allows further shifting of the hyperbolic transition to larger wavelengths.

We gratefully acknowledge financial support from the German Research Foundation (DFG) via SFB 986 "M$^3$," project C1.

[1]W. Cai and V. Shalaev, *Optical Metamaterials: Fundamentals and Applications* (Springer, New York, 2010).
[2]D. R. Smith and D. Schurig, Phys. Rev. Lett. **90**, 77405 (2003).
[3]D. R. Smith, W. J. Padilla, D. C. Vier, S. C. Nemat-Nasser, and S. Schultz, Phys. Rev. Lett. **84**, 4184 (2000).
[4]Y. Guo, W. Newman, C. L. Cortes, and Z. Jacob, Adv. OptoElectron. **2012**, 9.
[5]R. Wangberg, J. Elser, E. E. Narimanov, and V. A. Podolskiy, J. Opt. Soc. Am. B **23**, 498 (2006).
[6]S.-A. Biehs, M. Tschikin, R. Messina, and P. Ben-Abdallah, Appl. Phys. Lett. **102**, 131106 (2013).
[7]O. Kidwai, S. V. Zhukovsky, and J. E. Sipe, Phys. Rev. A **85**, 53842 (2012).
[8]A. J. Hoffman, L. Alekseyev, S. S. Howard, K. J. Franz, D. Wasserman, V. A. Podolskiy, E. E. Narimanov, D. L. Sivco, and C. Gmachl, Nature Mater. **6**, 946 (2007).
[9]Z. Jacob, J.-Y. Kim, G. V. Naik, A. Boltasseva, E. E. Narimanov, and V. M. Shalaev, Appl. Phys. B **100**, 215–218 (2010).
[10]H. N. S. Krishnamoorthy, Z. Jacob, E. Narimanov, I. Kretzschmar, and V. M. Menon, Science **336**, 205 (2012).
[11]P. R. West, S. Ishii, G. V. Naik, N. K. Emani, V. M. Shalaev, and A. Boltasseva, Laser Photonics Rev. **4**, 795 (2010).
[12]G. V. Naik, J. Kim, and A. Boltasseva, Opt. Mater. Express **1**, 1090 (2011).
[13]S.-A. Biehs, M. Tschikin, and P. Ben-Abdallah, Phys. Rev. Lett. **109**, 104301 (2012).
[14]Y. Guo and Z. Jacob, Opt. Express **21**, 15014 (2013).
[15]G. V. Naik and A. Boltasseva, Metamaterials **5**, 1 (2011).
[16]G. V. Naik, J. L. Schroeder, X. Ni, A. V. Kildishev, T. D. Sands, and A. Boltasseva, Opt. Mater. Express **2**, 478 (2012).
[17]P. B. Johnson and R. W. Christy, Phys. Rev. B **6**, 4370 (1972).
[18]Optical Society of America, "Optical properties of materials, nonlinear optics, quantum optics," in *Handbook of Optics*, edited by M. Bass (McGraw-Hill Professional, New York, 2009), Vol. 4.
[19]E. D. Palik, *Handbook of Optical Constants of Solids* (Academic Press, Boston, 1985).
[20]X. Wang, K.-p. Chen, M. Zhao, and D. D. Nolte, Opt. Express **18**, 24859 (2010).
[21]V. P. Drachev, U. K. Chettiar, A. V. Kildishev, H.-K. Yuan, W. Cai, and V. M. Shalaev, Opt. Express **16**, 1186 (2008).
[22]Y. Guo, C. L. Cortes, S. Molesky, and Z. Jacob, Appl. Phys. Lett. **101**, 131106 (2012).
[23]O. Kidwai, S. V. Zhukovsky, and J. E. Sipe, Opt. Lett. **36**, 2530 (2011).
[24]I. Iorsh, A. Poddubny, A. Orlov, P. Belov, and Y. S. Kivshar, Phys. Lett. A **376**, 185 (2012).
[25]Optical Society of America, "Devices, measurements, and properties," in *Handbook of Optics*, edited by M. Bass (McGraw-Hill Professional, New York, 1994), Vol. 2.